Uniaxial pressure effects in the cubic phase of K_2OsCl_6

1996 J. Phys.: Condens. Matter 8 5621

(http://iopscience.iop.org/0953-8984/8/30/011)

J. Phys.: Condens. Matter **8** (1996) 5621–5635. Printed in the UK

Uniaxial pressure effects in the cubic phase of K_2OsCl_6

Pablo J Prado and Robin L Armstrong

Department of Physics, University of New Brunswick, Fredericton, New Brunswick, Canada E3B 5A3

Received 28 February 1996, in final form 2 May 1996

Abstract. Chlorine nuclear quadrupole resonance (NQR) measurements of the effect of the application of uniaxial pressure applied along the (100) and (111) directions in single crystals of K_2OsCl_6 are reported at 78.0 K. The free induction decay times decrease with pressure due to the additional strains introduced. The corresponding frequency domain spectra indicate that the inhomogeneous broadening of the NQR signals is dominated by point defects, but that the nature, number and/or distribution of these defects is different in the two crystals. The spin–spin relaxation times are dependent on the crystal orientation and are independent of pressure. The measured T_2-results agree with calculated values. Spin–lattice relaxation data further illustrate the difference between the two crystals. It is described by a single exponential for the (111) crystal, but by a double exponential for the (100) crystal. The latter behaviour indicates the presence of dynamic clusters some 30 K above the temperature of the phase transition. The application of pressure is seen to hinder their formation.

1. Introduction

Extensive nuclear quadrupole resonance, neutron scattering, and optical spectroscopic studies of the structural and dynamic characteristics of antifluorite crystals have been reported. The work has been summarized in several review articles (Armstrong 1975, 1980, 1989a, b, Armstrong and van Driel 1975).

These experiments have provided an understanding of the mechanism responsible for the cubic- (O_h^5) to-tetragonal (C_{4h}^5) phase transition occurring in these compounds, specifically in K_2ReCl_6 and K_2OsCl_6. The structural phase transitions occurring in these compounds have, by inelastic neutron scattering measurements, been shown to be driven by the softening of the rotary lattice mode. A considerable number of chlorine nuclear quadrupole resonance (NQR) studies of K_2OsCl_6 have been undertaken; it is the ideal antifluorite compound for NQR investigation because it exhibits a narrow line and thus a strong signal. This work has shown that the softening of the rotary mode is accompanied by the development of precursor dynamic tetragonal phase clusters in the cubic phase. NQR, because it is a local probe, is particularly sensitive to the establishment of local order.

The high sensitivity of the NQR technique to perturbations in the local electric field gradients caused by the presence of point defects or dislocations, or by the application of pressure, makes it an ideal probe for the study of the subtleties associated with structural phase transitions. It has been used to study the effect of applied hydrostatic pressure on the phase transition in K_2OsCl_6 (Krupski and Armstrong 1989, Armstrong *et al* 1990). It is therefore an appropriate technique to choose to investigate the effect of uniaxial pressure on the same phase transition.

0953-8984/96/305621+15$19.50

Section 2 provides a discussion of the apparatus, samples and techniques used to study two single crystals of K_2OsCl_6 at 78.0 K. A novel uniaxial pressure device is described. ^{35}Cl free induction decay measurements are presented and discussed in section 3, spin–spin relaxation measurements in section 4, and spin–lattice relaxation time measurements in section 5. The conclusions are summarized in section 6.

2. The apparatus, samples, and techniques

A Tecmag Fourier transform pulse spectrometer was used to measure the ^{35}Cl NQR signals in the K_2OsCl_6 crystals. The experiments were carried out at 78.0 K because of the ease of maintaining a stable temperature using a liquid nitrogen bath.

A new uniaxial pressure device was developed based in part on ideas of Zamar *et al* (1983) and Berlinger and Müller (1977). The design, shown in figure 1, incorporates an easy-to-calibrate force arm and an easy-to-access sample space. The brass chamber which contains the rf coil mounted on a 1 cm long glass tube is immersed in a liquid nitrogen Dewar. The rf voltage is fed to the coil by a 50 Ω coaxial line, in this application at a frequency of 16.877 90 MHz. Two copper–constantan thermocouples were positioned at the top and bottom inside surfaces of the vessel to measure the temperature gradient. Measured temperature differences were in all cases less than 0.1 K. A Lake Shore temperature sensor located about 2 mm from the sample was used to monitor the temperature stability in the vicinity of the crystal. Variations were less than 0.1 K over the course of each experiment.

Pressure is exerted on the crystal surfaces by means of two polished glass cylinders. The top cylinder is attached to the pressure rod with a Teflon separator to provide thermal and electric isolation. The Teflon washers used to align the pressure rod in the stainless-steel tube are a loose fit to minimize friction. The bottom cylinder is seated on a pivot through Teflon and brass supports. The use of this pivot prevents strains from being exerted on the crystal which could cause it to break. The force applied by the horizontal bar is easy to calibrate because of the lever mechanism.

Helium gas is pumped into the system in order to avoid air condensation around the moving parts. The helium pressure is kept slightly above atmospheric; a balloon is used as a gauge.

Two single crystals of K_2OsCl_6, grown by S Mroczkowski at Yale University, were used for the experiments. The crystals were cut so as to have (100) and (111) planes, top and bottom. These faces were polished with fine sandpaper and finally with a slightly wet cloth. The sides of the crystals were cut to be normal to (100) and (111) faces. The final volumes of the crystals with the polished (100) and (111) faces were 0.045 and 0.041 cm^3, respectively. Henceforth, the two samples will be referred to as the (100) and the (111) crystals.

For each experiment the sample was allowed to equilibrate for 24 h at liquid nitrogen temperature before measurements were begun. The temperature was 78.0 ± 0.1 K. Measurements were taken for seven pressures in the range 0 to 9 MPa. The upper limit for the pressure was dictated by the strength of the antifluorite crystals. For pressures significantly greater than 9 MPa the crystals fractured. The pressure was applied in steps, starting without load, adding load up to the maximum value, and then removing it to return to the initial situation. By this procedure it was confirmed that the application of the pressure was a reversible process, and that the crystals were not damaged in the course of the experiments. Free induction decay (FID) signals following a single $\pi/2$ pulse were averaged over 200 acquisitions. Spin–spin relaxation (T_2-) times were deduced from maximum echo amplitudes following a $\pi/2$–$\tau/2$–π sequence for a series of τ-values; 80 scans were taken

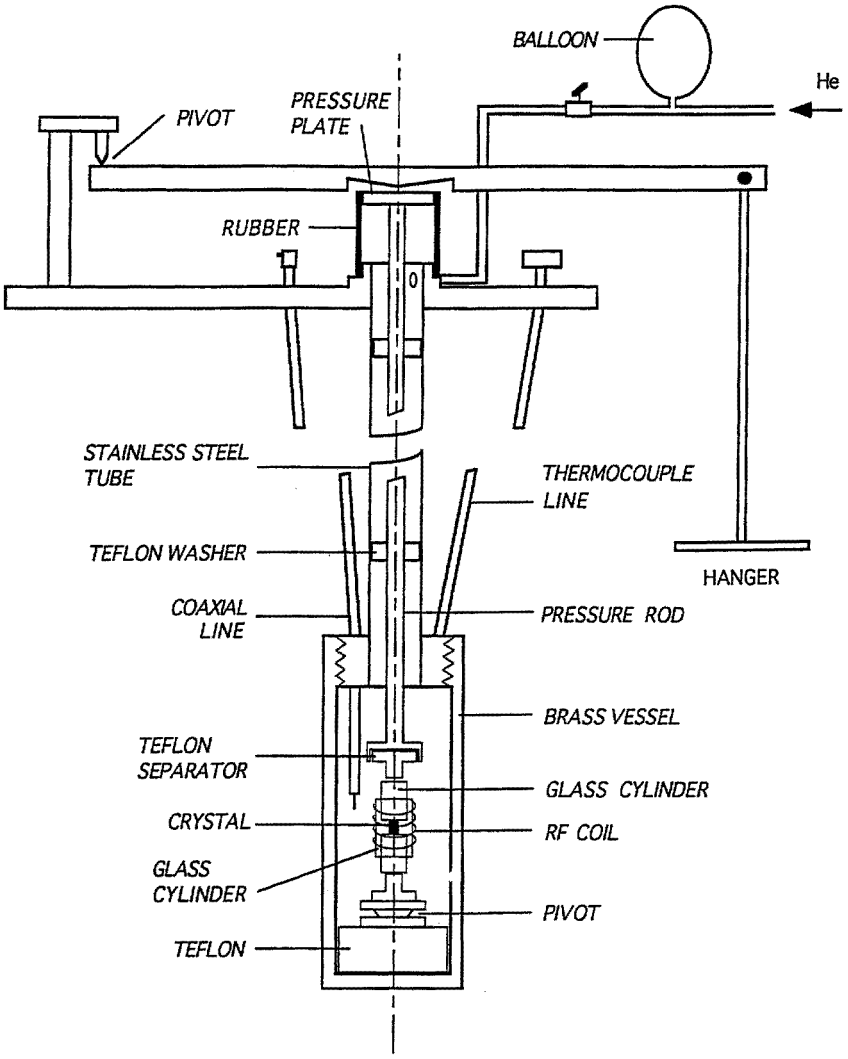

Figure 1. Uniaxial pressure device.

for each value of τ. Spin–lattice relaxation (T_1-) times were obtained from a π–τ–$\pi/2$ inversion recovery sequence. A series of τ-values were carefully chosen to cover the time-scales of both the expected fast and slow decays (Martin and Armstrong 1975, Armstrong *et al* 1986); 80 scans were taken for each value of τ.

3. Free induction decay measurements

Figure 2 shows a typical ^{35}Cl free induction decay signal. The actual data presented are for the (111) crystal at a pressure of 2.9 MPa. The line through the data is a least-squares fit to the function

$$M = M_0 \exp(-t/T_2^*) + B.$$

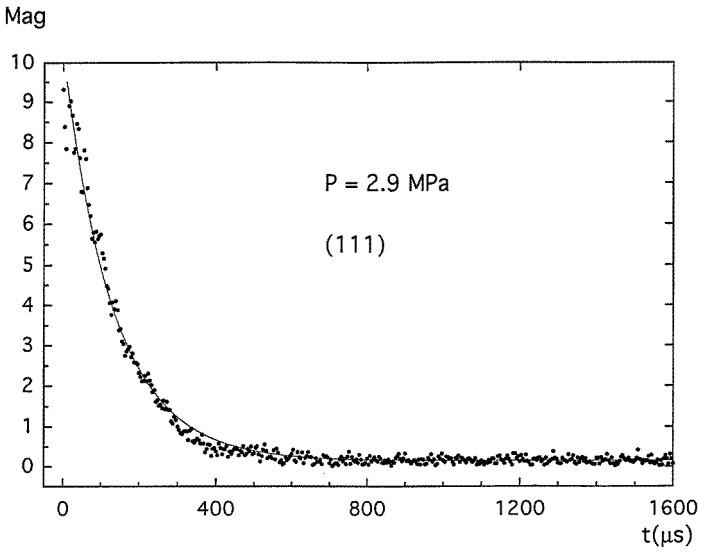

Figure 2. A typical ^{35}Cl free induction decay signal. The solid line through the data is a least-squares fit.

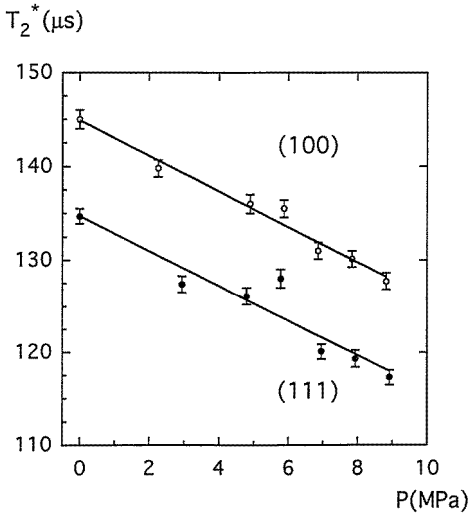

Figure 3. T_2^*-values obtained from fits to the free induction decay signals.

The values of T_2^* obtained from fits of this type to all of the data are shown in figure 3. The lines through the data are linear least-squares fits. We see from the graph that the value of T_2^* at zero applied pressure is different for the two crystals. This illustrates that the two crystals are not identical; they have different internal strains because of different defects or dislocations. We also see that in each case T_2^* decreases in a linear fashion as uniaxial pressure is applied over this low-pressure range. A decrease is to be expected as the application of the pressure will introduce additional strains.

The free induction decays were Fourier transformed to obtain amplitude spectra. These

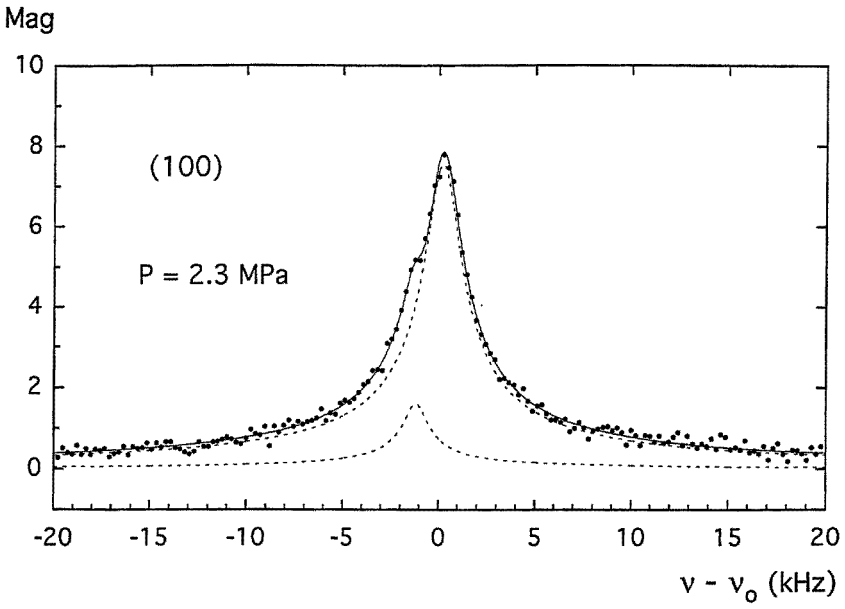

Figure 4. A typical example of an inhomogeneously broadened ^{35}Cl resonance line as obtained by Fourier transformation of a free induction decay signal. The dashed lines are the symmetric Lorentzian components; the solid line their vector sum.

spectra in each case consist of an asymmetric, inhomogeneous line that can be decomposed into two symmetric components. Figure 4 provides a typical example; it was obtained for the (100) sample under 2.3 MPa pressure. This behaviour has been reported previously for both powder samples (Ramia and Armstrong 1985) and single-crystal samples (Armstrong and Ramia 1985) of K_2OsCl_6. The behaviour has been explained in terms of the strains produced in the samples by the presence of point defects and dislocations (Stoneham 1969).

The decomposition of the asymmetric lines required five independent parameters, namely the central frequency and the line width of each component, and their relative intensity. Both pure Lorentzian line shapes, and combined Lorentzian–Gaussian line shapes were tried. In no case was the fit improved, or the parameters changed significantly, by adding a Gaussian component. It was concluded that the observed line shapes could be decomposed into two Lorentzian components consisting of a main line and a satellite shifted to a lower frequency. The dashed lines in figure 4 are the two symmetric components and the solid line is their vector sum.

The fact that the component lines can be represented by Lorentzian functions indicates that the inhomogeneous broadening in the present case is dominated by the presence of point defects in the crystals (Stoneham 1969). This result is in contrast with a previous experiment (Armstrong and Ramia 1985). In that case, the two component lines were of predominantly Gaussian character, indicating that the broadening was dominated by dislocations in the crystal. This difference illustrates that for a given crystal either point defects or dislocations can provide the dominant broadening mechanism. NQR is a sensitive probe of crystal imperfections.

Figure 5 is a plot of the peak frequencies of the main and satellite lines of the ^{35}Cl NQR spectra as a function of applied uniaxial pressure for both crystals. The lines through the data are least-squares fits. We see that in each case there is a small, but measurable, shift

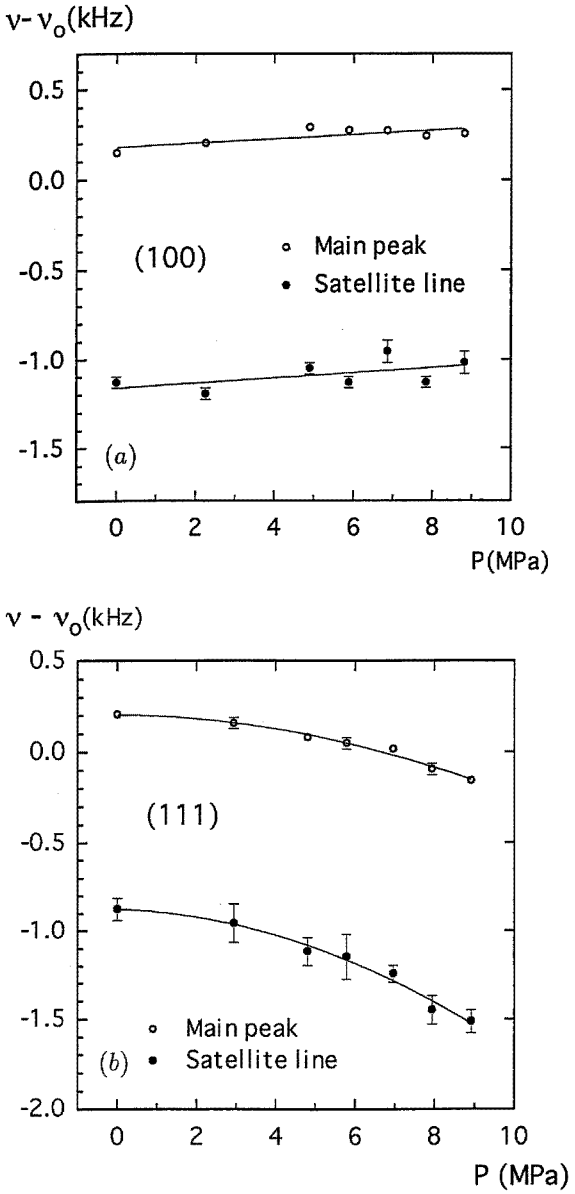

Figure 5. Peak frequencies of the main and satellite lines of the ^{35}Cl spectra as a function of applied uniaxial pressure. The solid lines are least-squares fits: (a) results for the (100) crystal; (b) results for the (111) crystal.

of frequency with pressure. The shift is to lower frequencies for the (111) crystal, and to higher frequencies for the (100) crystal. Note the high intrinsic accuracy of NQR frequency determinations. The maximum observed changes are about 400 Hz in 16.9 MHz, which is less than 1 part in 40 000.

Previous measurements of the effect of hydrostatic pressure on the ^{35}Cl NQR frequency in a powder sample of K_2OsCl_6 (Armstrong and Baker 1970) revealed a decrease in

frequency with increasing pressure. A value of $(\partial\nu/\partial P)_T = -0.7(5)$ kHz MPa^{-1} was reported. The explanation presented was that the application of pressure tends to destroy the π-bonding within the Cl–Os bonds. On the basis of this result, a frequency variation for the 0–9 MPa range of about 600 Hz is predicted. In the present case changes of about 400 Hz were observed for the (111) crystal and of about 100 Hz for the (100) crystal.

The difference in frequency shifts for the two crystals can be explained by taking account of the effects of a uniaxial pressure (Zamar and Brunetti 1988) which produce a perturbation in the electric field gradients which is a combination of contractions and dilations in different crystalline directions. For the (100) crystal, the ^{35}Cl nuclei associated with the Cl–Os bonds lying along the direction of the applied pressure are not observable in the NQR experiment. These bonds would experience the maximum effect of the pressure with the consequence that the π-bonding and associated averaged electric field gradient at the ^{35}Cl sites would be expected to decrease. On the other hand, the Cl–Os bonds perpendicular to the direction of the applied pressure would be significantly less affected by the pressure. Further, it is possible to imagine that in this case the sign of the effect would be reversed, resulting in a small increase in frequency with pressure.

Stoneham (1969) has presented a review of the calculation of the shapes of inhomogeneously broadened resonance lines in solids. These calculations permit a comparison of predicted line shapes and experimental measurements for each of the various broadening mechanisms. In the continuum approximation, and for a random distribution of defects, three different cases are identified. For strain broadening by straight-edge or screw dislocations the line shape is given by

$$I(\epsilon) = \pi^{-1} \int \mathrm{d}x \cos(\epsilon x) \exp\{-x^2(a - b[\ln x])\}$$

where ϵ is a normalized frequeny, and a and b are parameters which describe the dislocation characteristics. If $b = 0$, the line shape is a Gaussian; otherwise the line shape decreases faster than a Gaussian in the wings. For broadening by random electric fields the line shape is given by

$$I(\epsilon) = (2\pi)^{-1} \int \mathrm{d}x \exp(\mathrm{i}\epsilon x) \exp[-a|x|^{3/2}].$$

This is the Holtsmark distribution which is intermediate between a Lorentzian and a Gaussian. For broadening due to point defects by random strains and electric field gradients the line shape is given by the Lorentzian

$$I(\epsilon) = (2\pi)^{-1} \int \mathrm{d}x \exp[\mathrm{i}\epsilon x] \exp(-\alpha|x|)$$

where α is the half-width.

In order to explain the presence of a satellite line (Stoneham 1969) it is necessary to consider an inner region surrounding each of the centres responsible for the line broadening and in which the lattice is treated as discrete, as well as an outer region in which the continuum approximation is valid. When this is done, the final expression shows that $I(\epsilon)$ consists of a main line on which is superposed one or more satellite lines of the same shape but with different intensities as determined by details of the defects present.

Since the component lines of the observed profiles were Lorentzians, it follows that the cause of line broadening for the crystals studied is the presence of point defects. The results further show that the distribution of defects is altered by the application of the applied stress. The effect can be quantified by introducing the relative frequency shift

$$\Delta = (\nu_1 - \nu_2)/\nu_1$$

Table 1. Relative frequency shifts Δ between the main resonance and the satellite line.

Sample	$P = 0$	$P = 8.8$ MPa
(100)	7.5×10^{-5}	7.4×10^{-5}
(111)	5.5×10^{-5}	3.1×10^{-5}

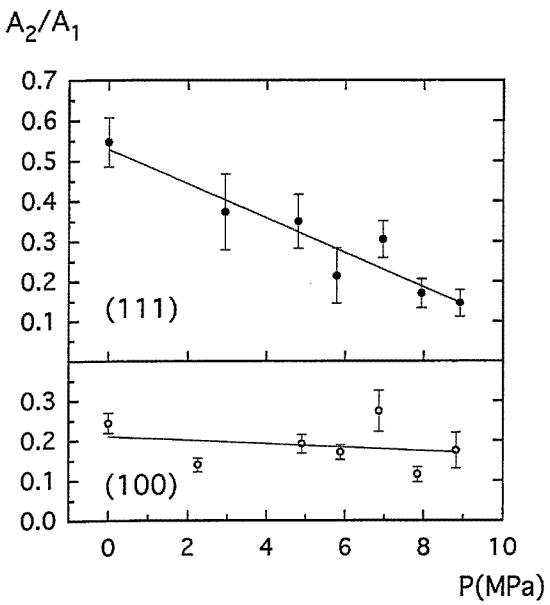

Figure 6. Changes in the relative intensities, A_2/A_1, of the satellite and main lines as a function of the applied uniaxial pressure. The solid lines are least-squares fits.

where ν_1 is the frequency of the line centre of the main resonance and ν_2 is the frequency of the line centre of the satellite. Values of Δ for no external stress and 8.8 MPa are presented in table 1. The difference in the values of Δ for no external stress is a result of differences in the two crystals. However, it is also seen that the effect of applied stress is much larger for the (111) crystal than for the (100) crystal. Since Δ depends not only on the positions of the defects, but also on the set of relevant internal variables that characterize it, any attempt to relate this parameter to a particular variable is unlikely to be profitable.

Figure 6 gives plots of the change in the relative intensity, A_2/A_1, of the satellite and the main peaks with applied pressure for the (100) and the (111) crystals. When comparing the two intensities a correction of about 5% was performed due to the small differences in line widths or T_2^*-values (Mintz and Armstrong 1980). The correction applied is

$$[A_2/A_1]_{corr} = [A_2/A_1]\exp[t_d(1/T_{2\,2}^* - 1/T_{2\,1}^*)]$$

where the subscripts 1 and 2 refer to the high- and low-frequency peaks, respectively, and $t_d = 36\ \mu$s is the delay time after the $\pi/2$ pulse. The solid lines are least-squares fits.

We see from figure 6 that A_2/A_1 for the (111) crystal decreases significantly as the applied pressure is increased, whereas the ratio is essentially independent of pressure for the (100) crystal. All other things being equal, we expect A_2/A_1 for the (111) crystal to change more rapidly with pressure than for the (100) crystal. The reason for this is probably the same one that explains the larger change in frequency for the (111) crystal as compared

to the (100) crystal. These changes are intimately connected to the alteration of the defect distribution.

But all other things are not equal for these two crystals as can be seen from a comparison of the values of A_2/A_1 for zero applied pressure. The values are dramatically different. This fact indicates that the point defects and/or their spatial distribution are quite different for the two crystals. This is somewhat surprising since the crystals were produced in the same laboratory using the same procedure. The result therefore suggests that the relative intensities of the two symmetric components of the asymmetric line are very sensitive to the exact nature, number, and/or distribution of the point defects.

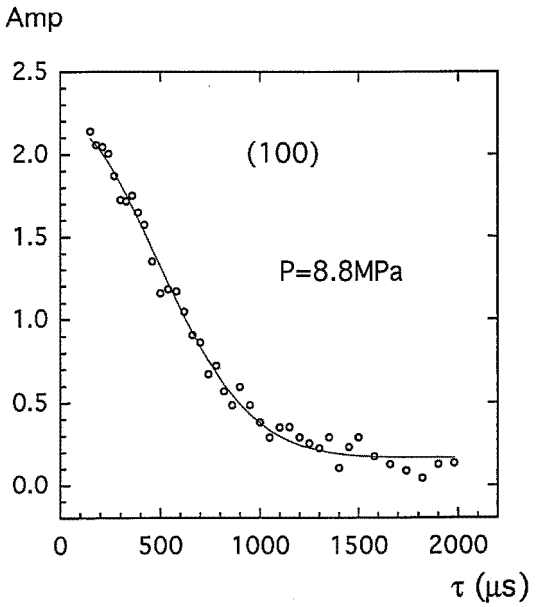

Figure 7. A representative ^{35}Cl decay signal as obtained following a spin-echo sequence. The Gaussian fit to the data yields the T_2-value.

4. Spin–spin relaxation time measurements

Spin–spin relaxation times, T_2, were deduced from the data acquired using the spin-echo sequence. The decay of the spin-echo amplitude as a function of the delay time τ yielded a Gaussian from which the value of T_2 was obtained. A representative decay is shown in figure 7. It was obtained for an applied pressure of 8.8 MPa. The spin-echo amplitude is plotted as a function of τ from which a T_2-value of 940 ± 20 μs is deduced from the expression

$$A = A_0 \exp(-2\tau^2/T_2^2).$$

Figure 8 is a plot of T_2 as a function of the applied pressure. We see that the values of T_2 are independent of pressure for the two samples. Because the ^{35}Cl NQR frequency changes with pressure, one might expect that T_2 would also change with pressure. However, the change of frequency is very small and is only observable because the high intrinsic NQR sensitivity. In comparison, the sensitivity to changes in T_2 is low. Therefore, there is no

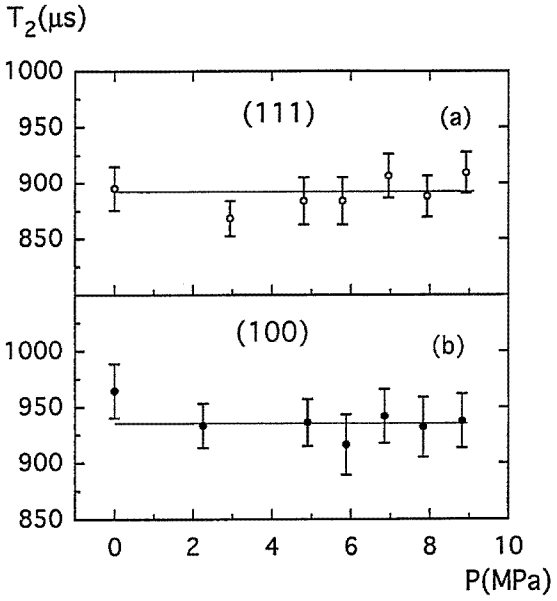

Figure 8. T_2-values as a function of applied uniaxial pressure. The solid lines are the average values.

inconsistency presented by the apparent constancy of the T_2-results. The averaged values of T_2 obtained for the two crystals are as follows: 937 ± 20 μs for the (100) crystal and 890 ± 20 μs for the (111) crystal.

Martin and Armstrong (1975) reported T_2-values in a powder sample of K_2OsCl_6 in the temperature range 45 to 300 K. No temperature dependence was apparent and an average T_2-value of 1017 ms was deduced. This result was compared to an estimated rigid-lattice second moment based on Van Vleck's (1948) formula and using equations given by Abragam and Kambe (1953) and Kano (1958) assuming a dipole–dipole interaction with the surrounding nuclei. The Os–Cl distance was taken to be a quarter of the lattice parameter and the calculation included up to third-nearest neighbours. The resultant value for T_2 is 1060 μs.

We have repeated the calculation using recently reported structural parameters (Prado *et al* 1995) and employing a computer program to include enough neighbouring nuclei to ensure four significant digits in the relaxation time output. A value of $T_2 = 899.1$ μs was obtained.

Second-moment calculations were carried out for single-crystal samples following the procedure described by Kano (1958), based on the symmetry of the K_2OsCl_6 cubic antifluorite structure. These calculations yielded T_2-values of 885.6 μs and 930.3 μs for the (111) and (100) orientations, respectively. These results are in excellent agreement with the experimentally measured values.

5. Spin–lattice relaxation measurements

Spin–lattice relaxation time (T_1-) data were obtained from the data acquired using an inversion–recovery sequence. Typical semi-logarithmic plots of the magnetization as a function of delay time τ are given in figures 9 and 10.

Data taken for 0 and 7.0 MPa applied pressure for the (111) crystal are shown in figure 9.

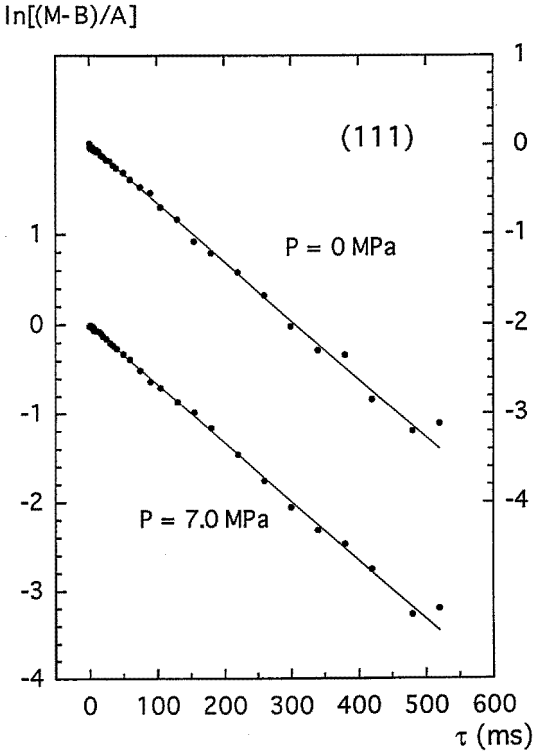

Figure 9. Typical semi-logarithmic decay plots obtained for the (111) crystal following an inversion–recovery sequence. The least-squares lines yield values of T_1.

These data indicate a pure exponential decay described by time constants $T_1 = 153 \pm 3$ μs and 151 ± 2 μs, respectively. This result is in agreement with previous measurements (Martin and Armstrong 1975). Similar behaviour is observed at all other pressures. The T_1-data are independent of applied pressure; the average value is calculated to be $T_1 = 152 \pm 3$ μs.

Data taken for 0 and 7.8 MPa applied pressure for the (100) crystal are shown in figure 10. These data are reminiscent of those obtained previously for powder and single-crystal samples of K_2OsCl_6 (Martin and Armstrong 1975, Armstrong *et al* 1986). They may be characterized by a double-exponential fit of the form

$$M(\tau) = A_L \exp(-\tau/T_{1L}) + A_S \exp(-\tau/T_{1S}) + B$$

where B includes both $M(\tau = \infty)$ and background contributions, and subscripts L and S refer to the long and short components of the decay, respectively. The parameters A_L and A_S are measures of the number of nuclei relaxing with time constants T_{1L} and T_{1S}, respectively. The T_{1L}-values were fitted first and then fixed to fit the T_{1S}-values. A visual inspection of figure 10 suggests that the T_{1L}- and T_{1S}-values at the two pressures are quite similar, but that the ratio A_S/A_L is different.

Figure 11 is a plot of the T_{1L}- and T_{1S}-values as a function of the applied pressure as obtained for the (100) crystal. These data indicate that the T_1-values are independent of pressure; the lines represent the average values, namely $T_{1L} = 141 \pm 3$ μs and $T_{1S} = 5.2 \pm 0.5$ μs.

Figure 12 is a plot of the ratio A_S/A_L as a function of the applied pressure. The data

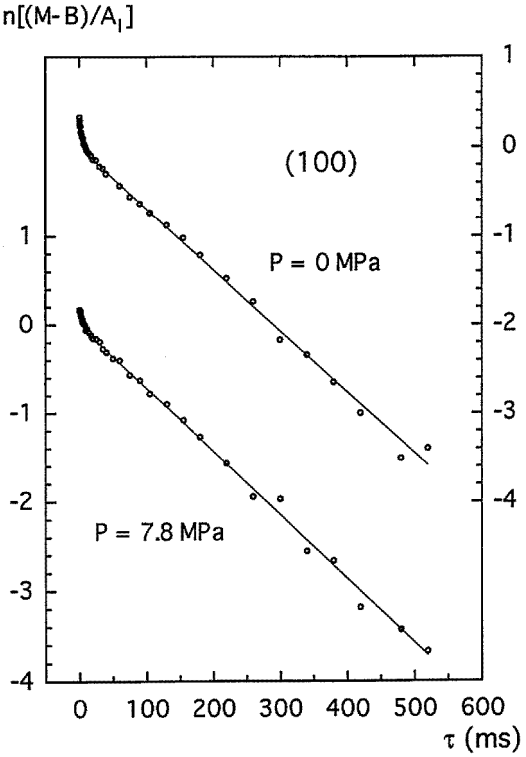

Figure 10. Typical semi-logarithmic decay plots obtained for the (100) crystal following an inversion–recovery sequence. These data are fitted by a double-exponential function and yield two time constants, T_{1S} and T_{1L}.

indicate a significant decrease in the ratio over the pressure range studied. They can be represented by a straight line with slope $-(2.4 \pm 0.1) \times 10^{-2}$ MPa^{-1}.

Previous work has shown that chlorine relaxation in K_2OsCl_6 is dominated by fluctuations of the electric field gradient having the symmetry of the rotary lattice mode, and that these fluctuations occur on two very different time-scales in localized regions of the sample (Armstrong *et al* 1986). The T_{1L}-component is the response to fluctuations on the time-scale of the lifetime of normal-mode excitations, whereas the T_{1S}-component is the response to fluctuations on the time-scale of the lifetime of the dynamic clusters that are the precursor to the structural phase transition that occurs at a lower temperature. The ratio A_S/A_L is a measure of the relative number of nuclei associated with dynamic clusters at 78.0 K. The fact that this ratio decreases with increasing pressure suggests that pressure tends to inhibit the formation of the dynamic clusters much as does the addition of impurities (Prado *et al* 1995). The fact that the data for the (111) crystal can be represented by a single exponential, which is equivalent to saying that A_S is zero, indicates that there is a significant difference in the point defects in the two crystals studied, and that in the case of the (111) crystal dynamic clusters have been totally suppressed by the defects at 78.0 K.

The observation that the various T_1-values measured are all independent of applied pressure suggests that the changes which must occur are too small to be detected with the sensitivity characteristic of this type of measurement.

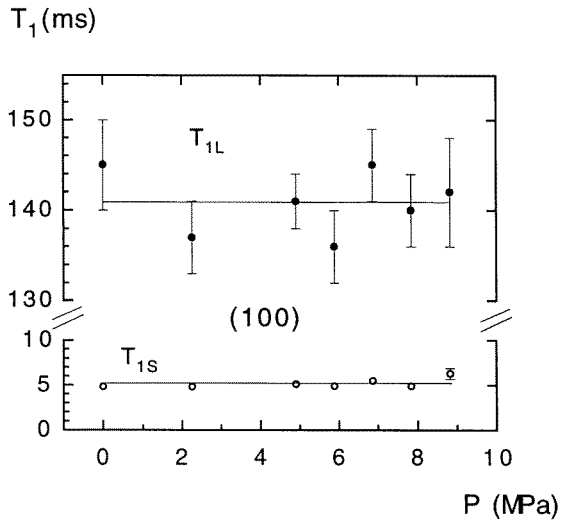

Figure 11. T_{1S}- and T_{1L}-values for the (100) crystal as a function of the applied uniaxial pressure. The solid lines are guides to the eye.

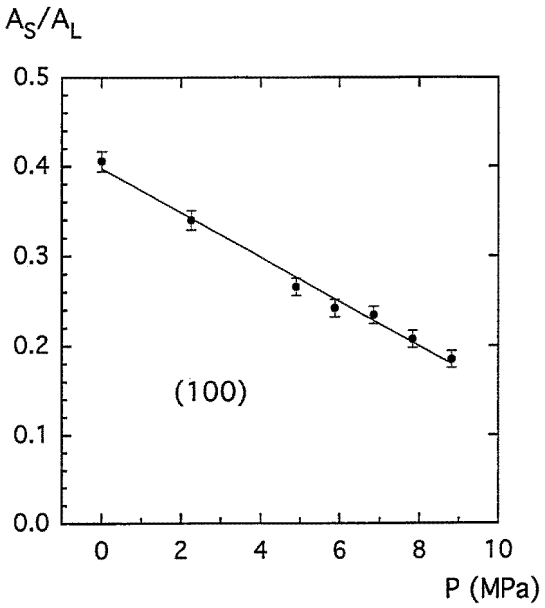

Figure 12. A plot of the amplitude ratio, A_S/A_L, of the two components of the double-exponential fit to the spin–lattice relaxation data for the (100) crystal. The solid line is a least-squares fit to these data.

6. Conclusions

A new design of uniaxial pressure cell has been presented and applied to the measurement of the ^{35}Cl NQR in single-crystal samples of K_2OsCl_6 at liquid nitrogen temperature.

Two single crystals were cut so that a uniaxial pressure could be applied perpendicular to (100) and (111) faces, respectively. Free induction decay signals, and spin–spin and spin–lattice relaxation measurements were carried out at seven different applied pressures in the range from 0 to 9 MPa.

The free induction decay times, T_2^*, decrease linearly with pressure due to the additional strains introduced by the application of the uniaxial pressure. The free induction decay signals were Fourier transformed to generate spectra in the frequency domain. In each case the spectra consisted of a single asymmetric line which was successfully decomposed into two Lorentzian lines. This result implies that the inhomogeneous broadening of the NQR signals is dominated by the presence of point defects. The central frequency of the main component is affected slightly by the pressure and by an amount that is consistent with the results of previous measurements of K_2OsCl_6 samples under hydrostatic pressure. The ratio of intensities of the two component peaks is different for the two samples at zero applied pressure. This is strong evidence that the nature, number, and/or distribution of the point defects is different in the two crystals. The different pressure dependences of this ratio are qualitatively understandable.

The spin–spin relaxation behaves as expected for a K_2OsCl_6 rigid lattice, and the relaxation times T_2 are independent of pressure. This is not surprising given the magnitude of the applied pressures and their small effect on the resonance frequencies. Second-moment calculations yield T_2-values in excellent agreement with the measured results for the (111) and (100) orientations.

The spin–lattice relaxation behaves dramatically differently for the two crystals; it is describable by a single exponential for the (111) crystal and by a double exponential for the (100) crystal. However, in previous experiments on single-crystal samples of K_2OsCl_6 both types of behaviour have been reported. The conclusion is that the two crystals used for the present experiments are significantly different. This agrees with the conclusion reached from a consideration of the line-shape data. All T_1-values measured are independent of pressure. This is as expected and is for the same reason that the T_2-values are independent of pressure. However, for the (100) crystal the amplitude ratio of the signals decaying with the short and long relaxation times, T_{1S} and T_{1L}, respectively, decreases with pressure. It is believed that this is evidence that the application of uniaxial pressure hinders the formation of dynamic precursor clusters much as does the addition of impurities to a sample.

Acknowledgments

This work was made possible by a Research Grant to RLA from the NSERC of Canada. The authors wish to thank Dr A Hamza for several useful discussions.

References

Abragam A and Kambe K 1953 *Phys. Rev.* **91** 894
Armstrong R L 1975 *J. Magn. Reson.* **20** 214
——1980 *Phys. Rep.* **57** 343
——1989a *Magnetic Resonance and Related Phenomena, 24th Ampere Congr. (Poznan, 1988)* (Amsterdam: Elsevier) p 54
——1989b *Prog. NMR Spectrosc.* **21** 151
Armstrong R L and Baker G L 1970 *Can. J. Phys.* **48** 2411
Armstrong R L, Krupski M and Su S 1990 *Can. J. Phys.* **68** 88
Armstrong R L and Ramia M E 1985 *J. Phys. C: Solid State Phys.* **18** 2977
Armstrong R L, Ramia M E and Morra R M 1986 *J. Phys. C: Solid State Phys.* **19** 4363

Armstrong R L and van Driel H M 1975 *Advances in Nuclear Quadrupole Resonance* vol 2 (New York: Heyden) p 179
Berlinger W and Müller K A 1977 *Rev. Sci. Instrum.* **48** 1161
Kano K 1958 *J. Phys. Soc. Japan* **13** 975
Krupski M and Armstrong R L 1989 *Can. J. Phys.* **67** 566
Martin C A and Armstrong R L 1975 *J. Magn. Reson.* **20** 411
Mintz J D and Armstrong R L 1980 *Can. J. Phys.* **58** 657
Prado P J, Armstrong R L and Powell B 1995 *Can. J. Phys.* **73** 626
Ramia M E and Armstrong R L 1985 *Can. J. Phys.* **63** 350
Stoneham A M 1969 *Rev. Mod. Phys.* **41** 82
Van Vleck J H 1948 *Phys. Rev.* **74** 1168
Zamar R C and Brunetti A H 1988 *Phys. Status Solidi* b **150** 245
Zamar R C, Brunetti A H and Pusiol D J 1983 *J. Mol. Struct.* **111** 171